Hybridisation effects in UPt_2Si_2

1990 J. Phys.: Condens. Matter 2 4059

(http://iopscience.iop.org/0953-8984/2/18/003)

J. Phys.: Condens. Matter 2 (1990) 4059–4066. Printed in the UK

Hybridisation effects in UPt_2Si_2

R A Steeman†, E Frikkee†, S A M Mentink‡, A A Menovsky‡§, G J Nieuwenhuys‡ and J A Mydosh‡

† Netherlands Energy Research Foundation ECN, PO Box 1, 1755 ZG Petten, The Netherlands

‡ Kamerlingh Onnes Laboratorium der Rijksuniversiteit Leiden, PO Box 9506, 2300 RA Leiden, The Netherlands

§ Natuurkundig Laboratorium der Universiteit van Amsterdam, Valckenierstraat 65, 1018 XE Amsterdam, The Netherlands

Received 12 June 1989, in final form 24 November 1989

Abstract. The intermetallic compound UPt_2Si_2 has been investigated by neutron diffraction, resistivity and specific heat measurements. An antiferromagnetic phase transition was observed at 35 ± 1 K. The ordered U moments are $(1.67 \pm 0.04)\mu_B$ at 4.2 K and form ferromagnetic *a–b* planes which are antiferromagnetically stacked in the *c* direction. The resistivity measurements revealed a large anisotropy between the *a* and *c* axes which significantly increases below T_N. At low temperatures the specific heat can be described by a linear electronic contribution with $\gamma = 32 \pm 1$ mJ mol^{-1} K^{-2} and a cubic lattice term with $\Theta_D = 271 \pm 5$ K. This description breaks down for $T > 40$ K. Analysis of the data with a different model, consisting of both Debye and Einstein modes, suggests a strong increase in γ.

1. Introduction

In recent years the UT_2Si_2 compounds with T a 3d, 4d or 5d transition metal have attracted much interest because of the variety of behaviours at low temperatures. Systematic studies [1–3] have revealed that at higher temperatures ($T > 200$ K) all these compounds exhibit local-moment behaviour with well defined U moments in the range from $2.6\mu_B$ to $3.6\mu_B$. This uniformity does not extend to low temperatures, where the compounds can be divided into three classes.

(I) Local-moment systems show ferromagnetic or antiferromagnetic ordering with U moments ranging from $1.4\mu_B$ for UCo_2Si_2 to $2.9\mu_B$ for UNi_2Si_2 [2].

(II) Pauli paramagnets do not order magnetically at low temperatures, and for these a temperature-independent susceptibility is observed (e.g. URe_2Si_2 and UOs_2Si_2 [1]).

(III) In systems in the intermediate regime between (I) and (II), heavy-fermion behaviour is found. An example of such a system is URu_2Si_2. In this compound, antiferromagnetic ordering takes place below $T_N = 17.5$ K with very small magnetic moments ($0.03\mu_B$). Below $T_c = 1$ K, superconductivity is found to coexist with the magnetic ordering. The heavy-fermion behaviour is characterised by the enhancement of both the electronic specific heat and the susceptibility [4, 5].

0953-8984/90/184059 + 08 $03.50

The transformation from localised (I) to itinerant (II) magnetism in the 4d and 5d transition-metal series was found to be correlated with the decreasing number of d electrons and not with a decrease in the interatomic U–U distances. The U–U separation in these series is always larger than 0.4 nm, whereas the critical distance below which itinerant magnetism is expected according to the so-called Hill criterion is about 0.35 nm [6].

In the above classification, UPt_2Si_2 can be identified as a local-moment system (I) with an antiferromagnetic phase transition at low temperatures. From DC susceptibility measurements on polycrystalline samples [1, 7, 8] a high-temperature effective moment of $(3.18–3.37)\mu_B$/formula unit and a Curie–Weiss temperature in the range from −57 to −68 K were derived, depending on the temperature interval of the measurements. The antiferromagnetic transition was observed at 37 ± 1 K. Metamagnetic behaviour as suggested in [8] can be excluded, at least up to 5 T, on the basis of the magnetisation versus field curves at constant temperatures [8, 9], which show no deviations from linearity.

Nieuwenhuys [10] has shown that these magnetic properties can be explained reasonably well by a mean-field crystalline electric field (CEF) model based on a singlet–singlet–doublet–singlet level scheme. These calculations have been corroborated by inelastic neutron scattering results [11], which indeed yielded the presence of such a level scheme with singlets at 53 and 79 K and a doublet at 63 K above the singlet ground state.

In this paper we present results of neutron diffraction, specific heat and resistivity measurements on UPt_2Si_2. The resistivity measurements were performed on single crystals along the *a* and *c* axes to study the anisotropy. All experiments were performed in zero magnetic field.

2. Sample preparation

Three polycrystalline pellets were prepared from stoichiometric melts of the three constituents. One of these was used in the specific heat measurements. For the neutron diffraction experiments the three pellets were powdered and mixed. The total volume of the powdered sample was 7.1 cm^3. This sample was also used in the determination of the crystal-field energy level scheme described in [11]. A single crystal of UPt_2Si_2 was grown by a modified tri-arc Czochralski method [12]. This single crystal was used in the specific heat measurements. The resistivity was measured along the *a* and *c* axes on two bar-shaped samples of $1 \times 1 \times 3$ mm^3 cut from the single crystal by spark erosion.

3. Crystal structure

The crystal structure of UPt_2Si_2 was determined by means of neutron powder diffraction. Diffraction patterns were recorded at 293 and 4.2 K on diffractometer HB5 at the high-flux reactor at Petten, with a wavelength of 0.258 58 nm. Soller collimators of 30′ were placed between the reactor and monochromator and between the sample and the four detectors. Higher-order beam contamination was eliminated by means of a pyrolytic graphite filter. A few weak impurity lines in the diagrams could be ascribed to PtO and UPt_2. The data were analysed with the Rietveld profile refinement technique, using nuclear scattering lengths of 8.42 fm for U, 9.50 fm for Pt and 4.15 fm for Si. An overall temperature factor was used in the refinements. The magnetic form factor for U in the

Table 1. Results of the neutron powder diffraction data refinements. The standard deviations based on statistics are given in parentheses. $R = 100\sqrt{[\Sigma I(\text{obs}) - (1/c)\Sigma I(\text{calc})]^2/\Sigma I(\text{obs})}$.

T (K)	a (nm)	c (nm)	z (U)	z (Pt)	z (Si)	m (μ_B)	R_n (%)	R_m (%)
293	0.419 72 (1)	0.969 06 (3)	0.7485 (4)	0.3779 (3)	0.1335 (9)	—	3.54	—
4.2	0.419 99 (1)	0.964 56 (4)	0.7477 (5)	0.3769 (4)	0.1270 (12)	1.67 (4)	3.10	5.62

$5f^2$ configuration, applied in the analysis of the magnetic scattering at 4.2 K, was taken from [13].

Our analysis reveals that UPt_2Si_2 has a tetragonal ($CaBe_2Ge_2$) structure, space group P4/nmm, with U placed at $(\frac{1}{4}, \frac{1}{4}, z)$, Pt at $(\frac{3}{4}, \frac{1}{4}, 0)$ and $(\frac{1}{4}, \frac{1}{4}, z)$, and Si at $(\frac{3}{4}, \frac{1}{4}, \frac{1}{2})$ and $(\frac{1}{4}, \frac{1}{4}, z)$. The parameters resulting from the refinements of the diagrams recorded at 293 and 4.2 K are summarised in table 1. The length of the a axis is almost constant on cooling from room temperature to 4.2 K, whereas the length of the c axis decreases by 0.5%. This means that the atomic layers become more closely packed at low temperatures. The closer packing is most pronounced in the Si–Pt–Si layered structure in one half of the unit cell, due to the additional relatively large change in the z parameter of the Si at $(\frac{1}{4}, \frac{1}{4}, z)$.

In the diagram at 4.2 K, one additional line is observed at $2\theta = 36.44°$, and can be indexed as the magnetic (100) reflection. Moreover, the intensities of the (102) and (111) reflections have increased. From these observations we conclude that UPt_2Si_2 orders antiferromagnetically into a pattern of ferromagnetic a–b planes with the U moments perpendicular to the planes and alternating polarisation along the c axis. The calculated moment is $(1.67 \pm 0.04)\mu_B$ at 4.2 K. These results are in good agreement with the work of Ptasiewicz-Bąk *et al* [8], except the value for the ordered moment, which is about 12% lower than the value reported in [8].

The intensity of the magnetic (100) reflection was measured as a function of temperature on the triple-axis spectrometer HB3 with an incoming wavelength of 0.147 51 nm. Two Soller collimators of 30′ were placed between the reactor and the Zn(002) monochromator and between the sample and the detector. The intensity of the second-order nuclear (200) reflection was reduced to about 2.5% of the first-order (200) intensity by the use of a pyrolytic graphite analyser. Special care was taken to stabilise the sample temperature. Relaxation times up to several hours to reach the equilibrium sample temperature were measured by monitoring the intensity of the magnetic (100) reflection, during both heating and cooling. We ascribe this effect to the large specific heat of UPt_2Si_2 in the temperature region of interest (see below), the large amount of sample (7.1 cm^3 powder), and poor heat contact between the sample crystallites. After stabilisation, the temperature was constant within 0.1 K, and the profile of the magnetic (100) reflection was measured. A Gaussian peak shape with a linear background was fitted to the data and the resulting maximum intensities are plotted as a function of temperature in figure 1. The relatively large temperature-independent intensity in this plot is due to second-order nuclear (200) reflection. (The (200) reflection is the strongest in the neutron powder diffractogram.) The Néel temperature deduced from these measurements was 34 ± 1 K.

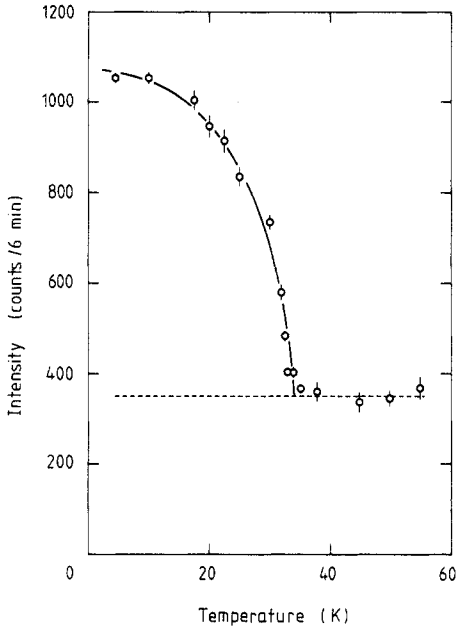

Figure 1. Temperature dependence of the maximum intensity of the magnetic (100) reflection of UPt_2Si_2: – – –, contribution of the second-order (200) reflection; ——, guide to the eye.

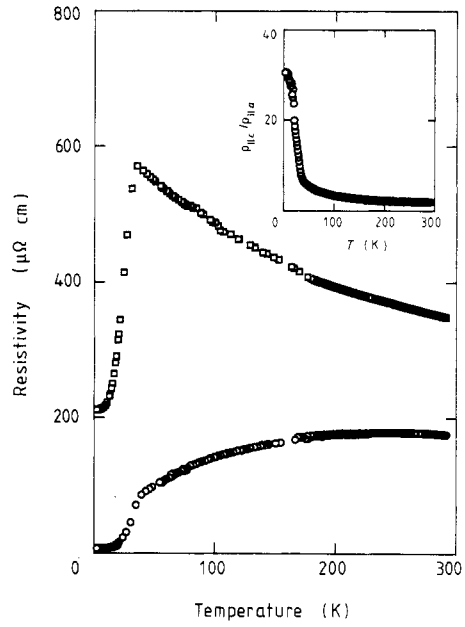

Figure 2. Resistivity of UPt_2Si_2 along the a (○) and c axes (□) as a function of temperature. The inset shows the temperature dependence of the anisotropy ρ_c/ρ_a.

4. Resistivity

The resistivity ρ was measured as a function of temperature along the a and c axes between 300 and 2 K. The voltage and current leads were attached to the samples with DAG1415 silver paint. The measurements were performed using a four-point probe method with a relative accuracy of about 0.5%, whereas the absolute values are correct only within 10% owing to uncertainties in the dimensions of the sample. As illustrated in figure 2, a large anisotropy is observed between the c and a axes. Along the c axis, the resistivity increases with decreasing temperature down to $T_N = 35 \pm 1$ K, where the resistivity drops sharply to about 60% of the room temperature resistivity at 2 K. On the other hand, parallel to the a axis, $d\rho/dT$ is positive already in the temperature range from about 250 K down to T_N. Below the phase transition, which is visible as a peak in $d\rho/dT$, the resistivity decreases rapidly. The resistivity at 2 K is only 4% of the value at room temperature. Hence, the ratio ρ_c/ρ_a changes drastically in the region of the antiferromagnetic phase transition from about 5 at 50 K to more than 30 for $T < 10$ K, whereas at room temperature this ratio is about 2 (inset, figure 2).

5. Specific heat

The specific heat of UPt_2Si_2 was measured in the temperature range between 2 and 186 K using the pulsed heating method. The data in figure 3 clearly show the antiferromagnetic phase transition at 35.0 ± 0.5 K. In order to analyse the specific heat at low temperatures

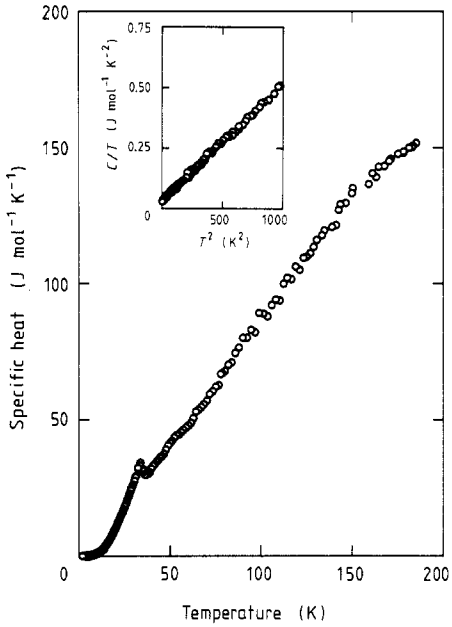

Figure 3. Specific heat of UPt_2Si_2 as a function of temperature. The inset shows the low-temperature part of the C/T versus T^2 plot after subtraction of the low-energy CEF contribution.

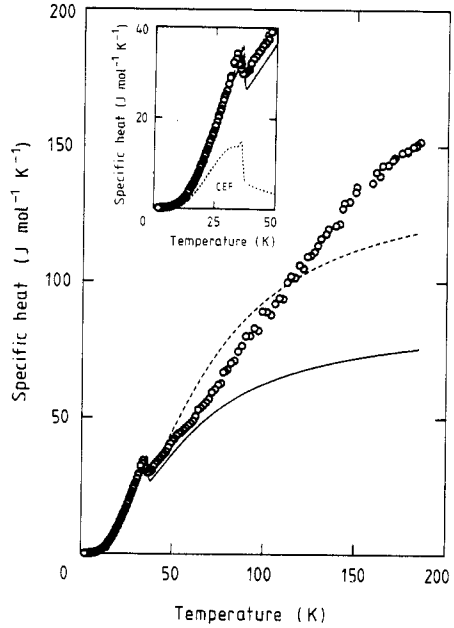

Figure 4. Fits of different models to the specific heat of UPt_2Si_2: ○, experimental data. The two curves represent the calculated specific heats with a linear electronic term with $\gamma = 32$ mJ mol^{-1} K^{-2}, a contribution from the low-energy CEF levels and a lattice term for 15 Debye modes with $\Theta_D = 271$ K (– – –) or nine Debye modes with $\Theta_D = 229$ K (——). The inset shows the low-temperature part on an expanded scale and depicts in addition the low-energy CEF contribution.

($T < 30$ K) the magnetic contribution due to the low-energy CEF levels was calculated in a mean-field approximation from the measured CEF level scheme [11] and subtracted from the measured data. The remaining low-T specific heat (inset, figure 3) could be described by a linear electronic contribution and a cubic lattice term (being the low-temperature limit of the Debye model for $3(1 + 2 + 2) = 15$ vibrational modes). The values obtained for γ and Θ_D were 32 ± 1 mJ mol^{-1} K^{-2} and 271 ± 5 K, respectively. This value for the Debye temperature is in good agreement with those found for other UT_2X_2 compounds [14].

An extrapolation of this model to higher temperatures ($T > 40$ K), in which the lattice specific heat was described by a Debye function with Θ_D taken from the low-temperature analysis, clearly showed that the simple Debye model is not applicable above 40 K. The results of this model are shown as the broken curve in figure 4. A possible explanation for this discrepancy is given below.

6. Discussion

The moment alignment along the c axis as observed in UPt_2Si_2 below $T_N = 35$ K, is a common feature among the UT_2Si_2 compounds exhibiting magnetic order (T ≡ Co, Ni,

Cu [2], T ≡ Pd, Rh [15], T ≡ Pt [8], T ≡ Ru [5]). In all these compounds the U moments form ferromagnetic *a–b* planes with the moments pointing perpendicular to these planes. However, the stacking of the planes may vary, as for T ≡ Cu (ferromagnetic), Rh, Ru, Pt, Co (antiferromagnetic) and for UNi_2Si_2 and UPd_2Si_2, in which the magnitude of the moments is modulated.

The formation of ferromagnetically coupled sheets with moments perpendicular to the planes has been described by Thayamballi and Cooper [16] and by Cooper *et al* [17] for the Ce and light actinide monopnictides. They calculated the interaction between two localised f electrons in a broad band of conduction electrons, starting from the Coqblin–Schrieffer [18] Hamiltonian. This interaction is mediated by the conduction electrons and is an extension of the well known RKKY interaction. It was shown that this interaction is strongly anisotropic and favours ferromagnetic coupling in planes perpendicular to the spin direction. Although the UT_2Si_2 compounds are more complex than those studied by Cooper *et al*, the presence of the ferromagnetic planes suggests the same type of exchange to be present in the UT_2Si_2 compounds. Accordingly, the oscillatory character of this RKKY-like interaction is probably responsible for the different stackings of the planes along the *c* axis in the various compounds.

From the difference in magnitude of the U moments at high temperatures ($3.2\mu_B$ [1, 7, 8]) and at 4.2 K ($1.67\mu_B$) we conclude that a strong hybridisation between the 5f electrons of U and the conduction electrons is present in this compound, leading to a Kondo-like reduction in the local U moment. This is further supported by our calculations based on the CEF level scheme presented in [11]. Starting from purely localised moments and using the mean-field approximation of [10], the U moment at 4.2 K was calculated to be $2.73\mu_B$, which is substantially larger than the value of $1.67\mu_B$ found from the neutron powder diffraction analysis. Note that both the Kondo effect and the Coqblin–Schrieffer interaction are consequences of this 5f–conduction electron (f–c) hybridisation. The variation in the relative strength of the Coqblin–Schrieffer and Kondo-like interactions, as a function of the f–c exchange J, would explain the variety in low-temperature behaviour in the UT_2Si_2 compounds (see, e.g., [18, 19]).

The Néel temperature deduced from the neutron scattering data agrees very well with the $T_N = 35 \pm 1$ K inferred from the specific heat and resistivity measurements. Good agreement is also found with the results of DC susceptibility experiments in a field of 2 T [1]. We thus conclude that the $T_N = 15$ K found from neutron diffraction experiments in zero field by Ptasiewicz-Bąk *et al* [8] is incorrect.

The resistivity along the *a* axis is much smaller than that along the *c* axis, indicating that the conduction mainly takes place within the layers parallel to the *a–b* plane. The same type of anisotropy is observed for UIr_2Si_2 [20]. A strikingly different behaviour is observed for URu_2Si_2 [21] and UFe_2Ge_2 [20], where the conduction is best along the *c* axis. The latter two compounds crystallise in the $ThCr_2Si_2$ structure (spacegroup I4/mmm), whereas UIr_2Si_2 and UPt_2Si_2 adopt the $CaBe_2Ge_2$ structure (P4/nmm). The main difference between these structures is the stacking of the atomic layers along the *c* axis, i.e. U–X–M–X–U–X–M–X–U (X ≡ Si, Ge; M ≡ Ru, Fe) for the $ThCr_2Si_2$ structure and U–M–X–M–U–X–M–X–U (M ≡ Pt, Ir; X ≡ Si) for the $CaBe_2Ge_2$ structure. Thus, in the $ThCr_2Si_2$ structure, the transition-metal atoms are separated from the U atoms by layers of silicon. If the positions of the transition-metal and silicon layers are interchanged (which in fact occurs in one half of the unit cell of the $CaBe_2Ge_2$ structure), the hybridisation between the 5f electrons of U and the d electrons of the transition metal will change, and this might cause the different anisotropies observed in the resistivities of these compounds [22].

As can be seen from the broken curve in figure 4, the low-temperature description of the specific heat could not be extended to temperatures above 40 K. The fact that the specific heat C_{calc} calculated from the low-temperature Debye model is larger than the observed value C_{obs} in the temperature range between 40 and 110 K indicates that this discrepancy cannot be explained from a simple enhancement of the electronic contribution, as observed in, for example, URu_2Si_2 [4]. It also cannot be due to the neglect of the high-energy CEF levels in the calculation of the CEF contribution to the specific heat, because here C_{calc} would be less than C_{obs}.

Therefore we propose a different model, in which the 15 Debye modes are replaced by nine Debye modes for the heavy atoms U and Pt, and six Einstein modes for the light Si atoms. Because of the large difference in masses, the characteristic temperature Θ_E of the Einstein modes should be much larger than Θ_D. In the low-temperature limit ($T < 0.1\Theta_E$), the contribution from the Einstein modes will be negligible and the $\gamma T + \beta T^3$ law is still valid. The resulting value for the Debye temperature is now 229 ± 4 K for the nine Debye modes (full curve in figure 4). Note that the Debye temperature remains high enough to validate the assumption that only the Debye modes need to be considered at low T ($0.1\Theta_E > 0.1\Theta_D = 23$ K). Extension of this model with only the nine Debye modes to $T > 40$ K reveals that now $C_{calc} \leqslant C_{obs}$ in the whole temperature range between 2 and 185 K (full curve in figure 4). The difference for $T > 40$ K can be ascribed to the contributions of the six Einstein modes, the high-energy CEF levels and an electronic contribution. The parameter γ in the electronic term must be temperature dependent because the low-temperature γ-value is far too small to explain the large measured value of the specific heat at 180 K. (It should be mentioned that this large specific heat has been confirmed in two independent measurements on a polycrystalline sample and a single crystal.) Independent of the model chosen for the different modes, the maximum lattice specific heat will never exceed $3R$ per atom (the Dulong and Petit law). For UPt_2Si_2 with five atoms in the unit cell, this limiting value is 124.7 J mol^{-1} K^{-1}. Furthermore, our calculations have shown that the maximum contribution of the high-energy CEF levels is less than 3.3 J mol^{-1} K^{-1}. Consequently, the remaining specific heat at 180 K, $\Delta C \geqslant 22$ J mol^{-1} K^{-1}, has to be due to the electrons. If we assume that the Fermi energy $E_F/k_B \gg 180$ K, a minimum value for the γ-coefficient of a linear electronic term at 180 K, $\gamma = 122$ mJ mol^{-1} K^{-2} can be deduced. Note that, for a reduction in E_F from heavy-fermion effects, the value for γ would be even larger. Unfortunately, the combined presence of the three different specific heat contributions (Einstein modes, CEF levels and an electronic term with a temperature-dependent γ) makes it impossible to obtain meaningful values for Θ_E, the high-energy CEF levels and γ from a fit to the experimental data.

An increase in γ above T_N is common for many heavy-fermion systems. However, to determine the exact value of γ and its temperature dependence in UPt_2Si_2, better knowledge of the phonon spectrum is required. Here neutron scattering measurements and specific heat data on a non-magnetic analogue would be of great help in resolving the electronic behaviour.

Acknowledgments

The authors acknowledge the help of Dr R B Helmholdt in the structure refinements, and Dr A J Dirkmaat for the stimulating discussions on the crystal-field problems. Part

of this work was supported by the Nederlandse Stichting voor Fundamenteel Onderzoek der Materie.

References

[1] Palstra T T M, Menovsky A A, Nieuwenhuys G J and Mydosh J A 1986 *J. Magn. Magn. Mater.* **54–7** 435
[2] Chelmicki L, Leciejewicz J and Zygmunt A 1985 *J. Phys. Chem. Solids* **46** 529
[3] Buschow K H J and De Mooij D B 1986 *Philips J. Res.* **41** 55
[4] Palstra T T M, Menovsky A A, Van den Berg J, Dirkmaat A J, Kes P H, Nieuwenhuys G J and Mydosh J A 1985 *Phys. Rev. Lett.* **55** 2727
[5] Broholm C, Kjems J K, Buyers W J L, Matthews P, Palstra T T M, Menovsky A A and Mydosh J A 1987 *Phys. Rev. Lett.* **58** 1467
[6] Hill H H 1970 *Plutonium and Other Actinides* ed W N Miner (New York: AIME) p 2
[7] Hiebl K and Rogl P 1985 *J. Magn. Magn. Mater.* **50** 39
[8] Ptasiewicz-Bąk H, Leciejewicz J and Zygmunt A 1985 *Solid State Commun.* **55** 601
[9] Palstra T T M 1986 *Thesis* Leiden
[10] Nieuwenhuys G J 1987 *Phys. Rev.* B **35** 5260
[11] Steeman R A, Frikkee E, Van Dijk C, Nieuwenhuys G J and Menovsky A A 1988 *J. Magn. Magn. Mater.* **76–7** 435
Note that reanalysis of the data has resulted in small shifts in the energies of the excited states
[12] Menovsky A A, Moleman A C, Snel G E, Gortenmulder T J, Tan H J and Palstra T T M 1986 *J. Cryst. Growth* **79** 316
[13] Wedgwood F A 1972 *J. Phys. C: Solid State Phys.* **5** 2427
[14] Endstra T, Dirkmaat A J, Mentink S A M, Menovsky A A, Nieuwenhuys G J and Mydosh J A 1990 *Physica* B submitted
[15] Ptasiewicz-Bąk H, Leciejewicz J and Zygmunt A 1981 *J. Phys. F: Met. Phys.* **11** 1225
[16] Thayamballi P and Cooper B R 1982 *J. Appl. Phys.* **53** 7902
[17] Cooper B R, Siemann R, Yang D, Thayamballi P and Banerjea A 1985 *Handbook on the Physics and Chemistry of the Actinides* ed A J Freeman and G H Lander (Amsterdam: North-Holland) p 435
[18] Coqblin B and Schrieffer J R 1969 *Phys. Rev.* **185** 847
Siemann R and Cooper B R 1980 *Phys. Rev. Lett.* **44** 1015
[19] Doniach J 1977 *Physica* B **91** 231
[20] Dirkmaat A J 1989 *Thesis* Leiden
[21] Palstra T T M, Menovsky A A and Mydosh J A 1986 *Phys. Rev.* B **33** 6527
[22] Steeman R A, Dirkmaat A J, Menovsky A A, Frikkee E, Nieuwenhuys G J and Mydosh J A 1990 *Physica* B at press